Am J Transl Res 2017;9(3):1317-1325
www.ajtr.org /ISSN:1943-8141/AJTR0040103

Original Article

Fasudil inhibits proliferation and collagen synthesis and induces apoptosis of human fibroblasts derived from urethral scar via the Rho/ROCK signaling pathway

Ning Xu[1*], Shao-Hao Chen[1*], Gen-Yi Qu[1*], Xiao-Dong Li[1], Wen Lin[2], Xue-Yi Xue[1], Yun-Zhi Lin[1], Qing-Shui Zheng[1], Yong Wei[1]

[1]Department of Urology, First Affiliated Hospital of Fujian Medical University, Fuzhou, China; [2]Department of Urology, Chinese PLA 476 Hospital, Fuzhou, China. [*]Equal contributors.

Received September 16, 2016; Accepted January 30, 2017; Epub March 15, 2017; Published March 30, 2017

Abstract: Fasudil has shown antifibrotic effects in various fibrotic diseases. However, its effects on human urethral fibroblasts are unknown. This study evaluated the effects of fasudil on cellular proliferation, migration, apoptosis, and collagen synthesis in human fibroblasts derived from urethral scar tissues. Human urethral scar fibroblasts were cultured by explant and incubated for 24 h or 48 h with fasudil (12.5, 25, 50 μmol/L) with or without transforming growth factor β1 (TGF-β1, 10 ng/mL), or left untreated (control). Cell proliferation and migration was determined by MTT assay and Transwell chambers, respectively. Apoptosis was measured by flow cytometry. Levels of α-smooth muscle actin (α-SMA), myosin light-chain phosphatase (MLCP), LIM domain kinase 1 (LIMK1), phospho-cofilin (p-cofilin), collagen I, and collagen III were determined by Western blot. Compared with the control group, TGF-β1 was associated with a significant increase in urethral fibroblast proliferation and migration, and α-SMA, MLCP, LIMK1, p-cofilin, collagen I, and collagen III levels. Compared with the control group, fasudil (with or without TGF-β1), significantly and negatively correlated, in a dose-dependent manner, with the proliferation and migration of urethral fibroblasts, as well as α-SMA, MLCP, LIMK1, p-cofilin, collagen I, and collagen III levels. Moreover, fasudil significantly induced apoptosis of fibroblasts induced by TGF-β1. Higher concentrations of fasudil (50 μmol/L) were associated with greater cell apoptosis without TGF-β1 stimulation compared with the normal control group. Fasudil, with or without TGF-β1 stimulation, may inhibit human urethral fibroblasts proliferation, migration, apoptosis, and collagen synthesis via the Rho/ROCK signaling pathway.

Keywords: Fasudil, Rho kinase inhibitor, urethral fibroblasts, extracellular matrix, collagen synthesis

Introduction

Urethral stricture is a common disease in urology, affecting 0.6%-0.9% of men [1, 2]. Urethral stricture leads to symptoms of the lower urinary tract [3] that negatively affect quality of life [4]. The most common etiologies are idiopathic, traumatic, inflammatory, or iatrogenic [5]. Surgical management of urethral stricture is challenging due to these multiple etiologies [6]. If the pathogenesis of the urethral stricture cannot be definitively decided, surgery or drug treatment will be unsatisfactory [7].

Urethral stricture is a narrowing of the urethra by scarring [8]. The pathological features of urethral stricture include excessive fibroblast proliferation, extracellular matrix deposition, and collagen synthesis [9-11]. RhoA (ras homolog gene family, member A) regulates actin filament remodeling in fibroblasts, and activates the Rho-associated protein kinase (ROCK)-dependent signaling pathway to promote the formation of stress fibers and scar contraction [12-14]. The promotion of ROCK of actomyosin-mediated contractility is through phosphorylation of LIM domain kinase 1 (LIMK1) and regulatory light chain of myosin II [15, 16]. In addition, ROCK regulates fibroblast proliferation, differentiation, and apoptosis [17, 18].

Fasudil, a small molecule inhibitor of ROCK, has been shown to have antifibrotic effects in various fibrosis diseases [19-22]. However, the effect of fasudil on urethral fibroblast proliferation, migration, and extracellular matrix deposi-

tion has not been evaluated. Injection of transforming growth factor beta 1 (TGF-β1) into the urethral wall of rats was shown to induce urethral fibrosis, relative to the effect of normal saline injection [23].

Here, we evaluated the effect of fasudil, with or without TGF-β1, on the proliferation, migration, apoptosis, and extracellular matrix synthesis of human urethral fibroblasts, focusing on the role of the Rho/ROCK signaling pathway in urethral scar.

Materials and methods

This study was approved by the Ethics Committee of Fujian Medical University and all patients provided written content.

Drug and reagents

Fasudil hydrochloride was purchased from Luoxin Biotechnology (Shanghai). TGF-β1 was obtained from Sigma-Aldrich. The following were purchased from Santa Cruz Biotechnology: monoclonal mouse anti-alpha smooth muscle actin (α-SMA); polyclonal goat anti-myosin light-chain phosphatase (MLCP); monoclonal rabbit anti-LIMK1; monoclonal rabbit anti-phospho-cofilin (anti-p-cofilin); polyclonal rabbit anti-collagen I; polyclonal rabbit anti-collagen III; polyclonal rabbit anti-glyceraldehyde-3-phosphate dehydrogenase (GAPDH) antibody; and horseradish peroxidase (HRP)-conjugated goat anti-rabbit antibody. Fetal bovine serum (FBS) and the Roche apoptosis detection kit were obtained from Bofeng Biological Technology.

Cell culture

Surgical specimens of urethral stricture tissues of 5 human patients (aged 25-31 y) were collected at the Department of Urology of First Affiliated Hospital of Fujian Medical University. None of the patients had received any drugs or radiation therapy before surgery.

Primary urethral scar fibroblasts were cultured from the surgical specimens by explant [24, 25]. Briefly, tissue specimens were cut into 0.5 mm^3 pieces under sterile conditions, repeatedly washed in Hanks' balanced salt solution (without Ca^{2+} or Mg^{2+}) containing penicillin (100 U/mL) and streptomycin (0.l μg/mL), and then cut into 1 mm × 1 mm × 1 mm pieces. The prepared specimens were digested by oscillation in 0.1% collagenase for 50 min at 37°C. After filtering through a 200-mesh cell screen, the cell suspensions were collected into a centrifuge tube and centrifuged at 1000 rpm for 5 min, and resuspended in Dulbecco's modified Eagle's medium (DMEM) supplemented with 20% inactivated fetal calf serum.

The survival rate of fibroblasts was approximately 95%, according to the trypan blue exclusion test. Primary urethral scar fibroblasts (1.0×10^6 cells/5 mL) were added to 500 mL culture flasks (37°C in 5% CO_2). When cells reached a monolayer, primary fibroblasts were passaged with 0.1% collagenase. Cells at passage 4-8 were used in the subsequent studies. Urethral scar fibroblasts were distinguished from other cells types based on positive staining of the fibroblast marker vimentin through immunohistochemical analysis [26].

Cell proliferation

Cell proliferation was analyzed by MTT (3-[4,5-dimethylthiazol-2-yl]-2,5-diphenyltetrazolium bromide) assay. Briefly, the fibroblasts were harvested during the logarithmic growth phase and seeded into 96-well plates at 5×10^4 cells per well, then incubated in DMEM containing 10% FBS for 24 h. After serum deprivation for 24 h, and fibroblasts were treated with various concentrations of fasudil (0, 6.25, 12.5, 25, 50, 100, or 150 μmol/L), wherein 0 μM was considered the control group, in the presence or absence of 10 ng/mL TGF-β1.

After incubation for 24 or 48 h, 20 μL of 5 mg/mL MTT was added into each well. The cultures were further incubated for 4 h before dimethyl sulfoxide (150 μL) was added to each well. The optical density of each well was determined at 570 nm using a microplate spectrophotometer (Shanghai Metash Instruments). The same experiment was duplicated 3 times. The concentrations of drugs were graphed (*x*-axis) against the mean optical density (*y*-axis). The growth inhibition rate was calculated as (1-mean optical density of treated cells/mean optical density of control cells) × 100%.

Cell migration assay

Transwell chambers were used to measure the migration ability of the cells. Briefly, Transwell

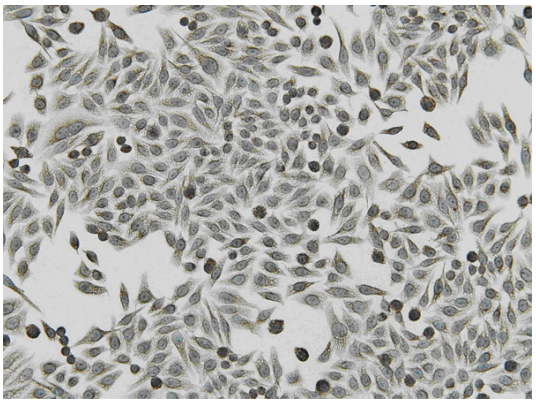

Figure 1. Immunohistochemical analysis demonstrated positive staining of fibroblast marker vimentin (200 ×).

chambers were placed in 24-well plates. The upper chambers were coated with 50 μL of Matrigel diluted with serum-free DMEM, and the lower chambers were filled with 500 μL of DMEM containing 10% FBS. Cells (1.0×10^5 cells per well) were resuspended in 100 μL of growth medium and added to the upper compartment of the chamber, then cells were treated with various concentrations of fasudil (0, 12.5, 25, or 50 μmol/L) in the absence or presence of 10 ng/mL TGF-β1. After incubation at 37°C for 12 h, the migrated cells on the lower face of the membrane were counted under a light microscope (Olympus, Japan) at 400 × magnification. The number of migrated cells from 10 randomly selected fields was counted and photographed, and then the mean number of cells was calculated.

Cell apoptosis

Flow cytometry was used to detect cell apoptosis. Cells were treated with various concentrations of fasudil (0, 12.5, 25, or 50 μmol/L) in the absence or presence of 10 ng/mL TGF-β1 for 24 h, then digested using 0.25% trypsin, and washed twice with phosphate-buffered saline. Cells were prepared as a single-cell suspension at 1×10^6 cells/mL and resuspended in 100 μL annexin V-FITC binding buffer, 5 μL propidium iodide (PI), or both in the dark for 30 min at room temperature; then 400 μL binding buffer was added to wash the annexin/PI stained cells. Untreated cells served as the negative control. The apoptotic fibroblasts were immediately analyzed using flow cytometer (Becton Dickinson, USA). Annexin V-FITC-positive and PI-negative cells were defined as apoptotic cells. The rate of apoptosis was calculated as the ratio of the number of Annexin V-positive cells to the number of PI-negative cells [27].

Western blot analysis

After 24 h of incubation with the various treatments, fibroblasts were collected and homogenized with radio immunoprecipitation assay (RIPA) lysis buffer, then centrifuged at 14,000 × g for 5 min. The protein concentrations were measured using a bicinchoninic acid protein assay. Protein samples (15 μg) was subjected to 10% sodium dodecyl sulfate-polyacrylamide gel electrophoresis and transferred onto polyvinylidene fluoride membranes. The membranes were blocked with 5% fat-free milk in TBST buffer. Afterward the membranes were serially incubated with the following primary antibodies: monoclonal mouse anti-α-SMA (1:200 dilution); polyclonal goat anti-MLCP (1:500 dilution); monoclonal rabbit anti-LIMK1 (1:1000 dilution); monoclonal rabbit anti-p-cofilin (1:1000 dilution); polyclonal rabbit anti-collagen I (1:400 dilution); polyclonal rabbit anti-collagen III (1:400 dilution); and polyclonal rabbit anti-GAPDH (1:400 dilution). After each incubation and washing, the membranes were incubated with HRP-conjugated goat anti-rabbit secondary antibody.

All the immunoreactive proteins were visualized using an electrochemiluminescence kit, in accordance with the manufacturer's instructions, and photographed. Band intensity was analyzed using Quantity One software version 4.6.2 (Bio-Rad, Hercules, USA). The relative protein levels were compared to that of GAPDH from the same sample.

Statistical analysis

Each experiment was performed in triplicate, and values are presented as mean ± standard deviation. Statistical analyses were carried out using SPSS software (Version 19.0; Chicago, USA). Differences in the inhibition rates, cell counts, apoptosis rates, and protein levels of paired groups were compared using the Mann-Whitney U or Kruskal-Wallis test. In all tests, two-sided *P*-values < 0.05 were considered statistically significant.

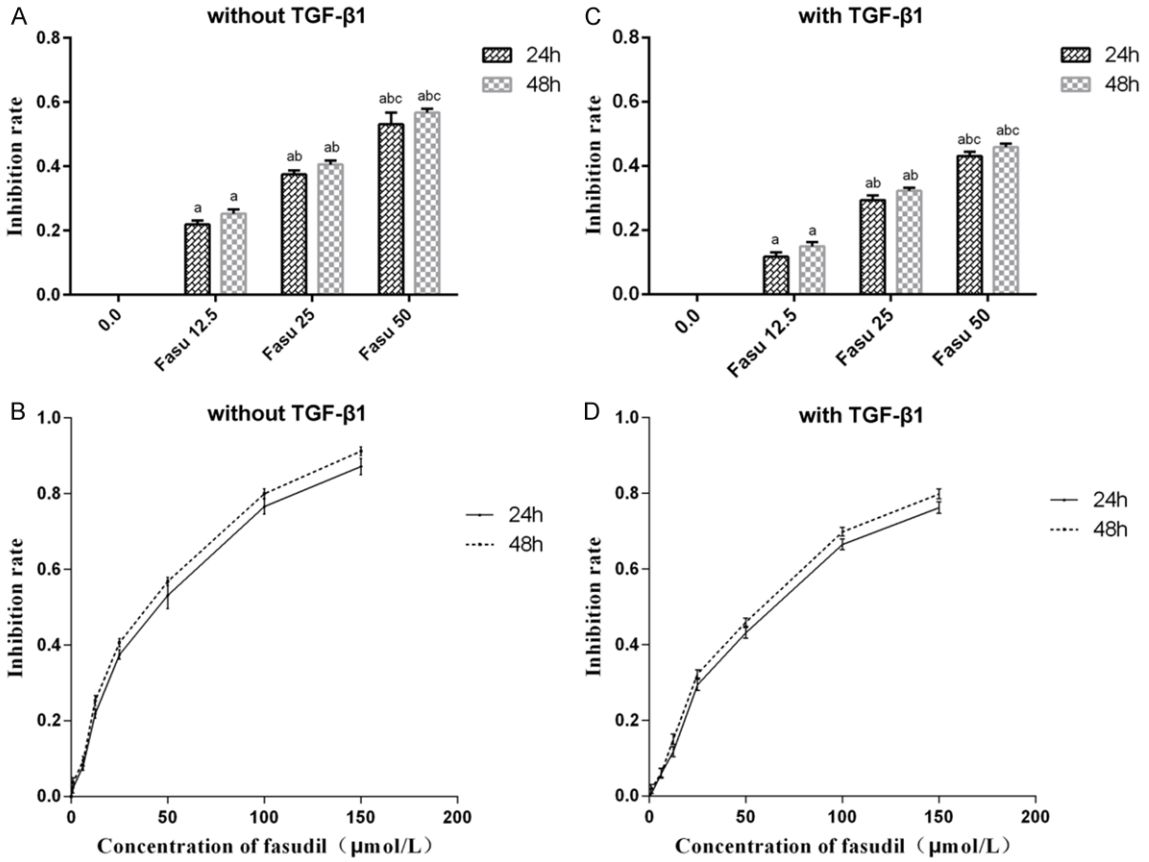

Figure 2. Effects of fasudil on fibroblast growth. Cells were treated with different concentrations of fasudil (0, 12.5 μmol/L, 25 μmol/L and 50 μmol/L) with or without TGF-β1 10 ng/mL for 24 and 48 h. Cell inhibition rate (%) in the absence (A) or presence (B) of TGF-β1 stimulation. Cell inhibition curve in the absence (C) or presence (D) of TGF-β1 stimulation. Cell growth was inhibited in a dose-and time-dependent manner. Data were expressed as mean ± SD (n = 3). [a]$P < 0.05$ cf. control group; [b]$P < 0.05$ cf. fasudil 12.5 μmol/L group; [c]$P < 0.05$ cf. fasudil 25 μmol/L group in A. [a]$P < 0.05$ cf. TGF-β1 group; [b]$P < 0.05$ cf. TGF-β1 + fasudil 12.5 μmol/L group; [d]$P < 0.05$ cf. TGF-β1 + fasudil 25 μmol/L group in B. The half-maximal inhibitory concentration (IC_{50}) of fasudil for inhibition of fibroblast growth was 58.09 and 50.93 μmol/L at 24 and 48 h, respectively. The IC_{50} of fasudil inhibiting fibroblast proliferation induced by TGF-β1 10 ng/mL was 38.49 and 32.95 μmol/L at 24 and 48 h, respectively.

Results

Characterization of cultured urethral scar fibroblasts

Under the inverted microscope, the non-adherent fibroblasts were spherical and the adherent fibroblasts were spindle-shaped or irregular polygonal with clear boundaries and regular long arrangements. Cells reached 80-90% confluence after 2 to 3 days of culture. Immunohistochemical analysis showed that the cultured cells exhibited positive staining for vimentin (**Figure 1**).

Effects of fasudil on proliferation of fibroblasts

The proliferation of cells was determined by the MTT assay after various treatments (**Figure 2**). Fasudil at concentrations of 6.25, 12.5, 25, and 50 μmol/L inhibited fibroblasts proliferation in a dose-and time-dependent manner compared with the normal control group ($P < 0.05$; **Figure 2A** and **2B**). The half-maximal inhibitory concentration (IC_{50}) of fasudil for inhibition of fibroblast growth was 58.09 and 50.93 μmol/L at 24 and 48 h, respectively. Fasudil at the tested concentrations also significantly inhibited fibroblast proliferation induced by 10 ng/mL TGF-β1 in a dose-and time-dependent manner compared with the TGF-β1 control group ($P < 0.05$; **Figure 2C** and **2D**). The IC_{50} of fasudil inhibiting fibroblast proliferation induced by TGF-β1 10 ng/mL was 38.49 and 32.95 μmol/L at 24 and 48 h, respectively. The inhibitory effect of fasudil on fibroblast proliferation

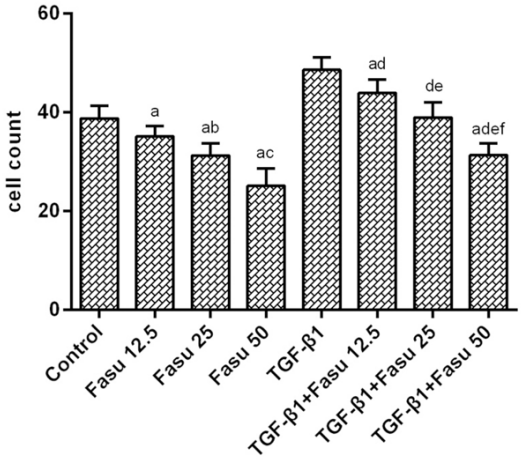

Figure 3. Effects of fasudil on fibroblast migration. Cells were treated with different concentrations of fasudil for 12 h. Transwell chambers assay was used to determine the cells migration. Data were expressed as mean ± SD (n = 3). [a]*P* < 0.05 cf. control group; [b]*P* < 0.05 cf. fasudil 12.5 μmol/L group; [c]*P* < 0.05 cf. fasudil 25 μmol/L group; [d]*P* < 0.05 cf. TGF-β1 group; [e]*P* < 0.05 cf. TGF-β1 + fasudil 12.5 μmol/L group; [f]*P* < 0.05 cf. TGF-β1 + fasudil 25 μmol/L group.

induced by TGF-β1 was more pronounced than the cells in the normal control group (*P* < 0.05).

Effects of fasudil on fibroblast migration

Cell migration was measured using the Transwell chambers assay (**Figure 3**). Treatment with fasudil without TGF-β1 was associated with a significantly lower number of migrated cells to 35.1 ± 2.1 at 12.5 μmol/L, to 31.2 ± 2.5 at 25 μmol/L, and to 25.1 ± 1.9 at 50 μmol/L compared with the normal control group (38.7 ± 2.6; all *P* < 0.05). TGF-β1 stimulation was associated with an increased number of migrated cells compared with the normal control group (48.6 ± 2.5 cf. 38.7 ± 2.6, *P* < 0.05). Moreover, fasudil in combination with TGF-β1 significantly reduced the number of migrated cells to 43.9 ± 2.7 at 12.5 μmol/L, to 38.9 ± 3.1 at 25 μmol/L, and to 31.3 ± 2.4 at 50 μmol/L, compared with the TGF-β1 control group (all *P* < 0.05). In the presence or absence of TGF-β1 stimulation, fasudil decreased the number of migrated cells in a dose-dependent manner.

Effects of fasudil on fibroblasts apoptosis

Fasudil without TGF-β1 at the concentration of 50 μmol/L significantly increased the rate of apoptosis compared with control group (7.96% ± 2.43% cf. 0.00% ± 0.01%, *P* < 0.05). Fasudil without TGF-β1 increased the rate of apoptosis to 9.96% ± 2.12% at 12.5 μmol/L, and to 11.21% ± 7.34% at 25 μmol/L. However, there were statistically significant differences in the rate of apoptosis between fasudil 12.5 μmol/L or 25 μmol/L and the normal control group (all *P* > 0.05). Fasudil in combination with TGF-β1 reduced the rate of apoptosis to 3.20% ± 1.27% at 12.5 μmol/L, to 16.86% ± 1.08% at 25 μmol/L, and to 19.88% ± 1.51% at 50 μmol/L, compared with the TGF-β1 control group (all *P* <0.05). In the presence of TGF-β1 stimulation, fasudil increased the rate of apoptosis in a dose-dependent manner (**Figure 4**).

Effects of fasudil on protein levels of α-SMA, MLCP, LIMK1, p-cofilin, collagen I, and collagen III

A representative α-SMA, MLCP, LIMK1, p-cofilin, collagen I, and collagen III protein band of Western blot analysis is shown in **Figure 5A**. TGF-β1 stimulation significantly increased the α-SMA, MLCP, LIMK1, p-cofilin, collagen I, and collagen III protein levels compared with the normal control group (all *P* < 0.05; **Figure 5B-G**). Whether in the presence or absence of TGF-β1 stimulation, fasudil at the tested dose significantly decreased α-SMA, MLCP, LIMK1, p-cofilin, collagen I, and collagen III protein expression in a dose-dependent manner.

Discussion

The current study showed that fasudil (12.5-50 μmol/L) significantly inhibited human urethral scar fibroblasts proliferation in the absence or presence of TGF-β1 stimulation in a dose- and time-dependent manner. Treatment with fasudil significantly suppressed fibroblast migration in a dose-dependent manner. Fasudil also significantly increased the apoptosis of fibroblasts under the stimulation of TGF-β1. Moreover, fasudil attenuated the expression of α-SMA, MLCP, LIMK1, p-cofilin, collagen I, and collagen III protein. These findings suggest that the therapeutic potential of fasudil in urethral strictures may partly be due to their inhibitory effect on fibroblast proliferation and collagen synthesis via suppression of the Rho/ROCK pathways.

Urethral scar fibroblasts are the main effector cell in the urethral stricture [28]. In the present

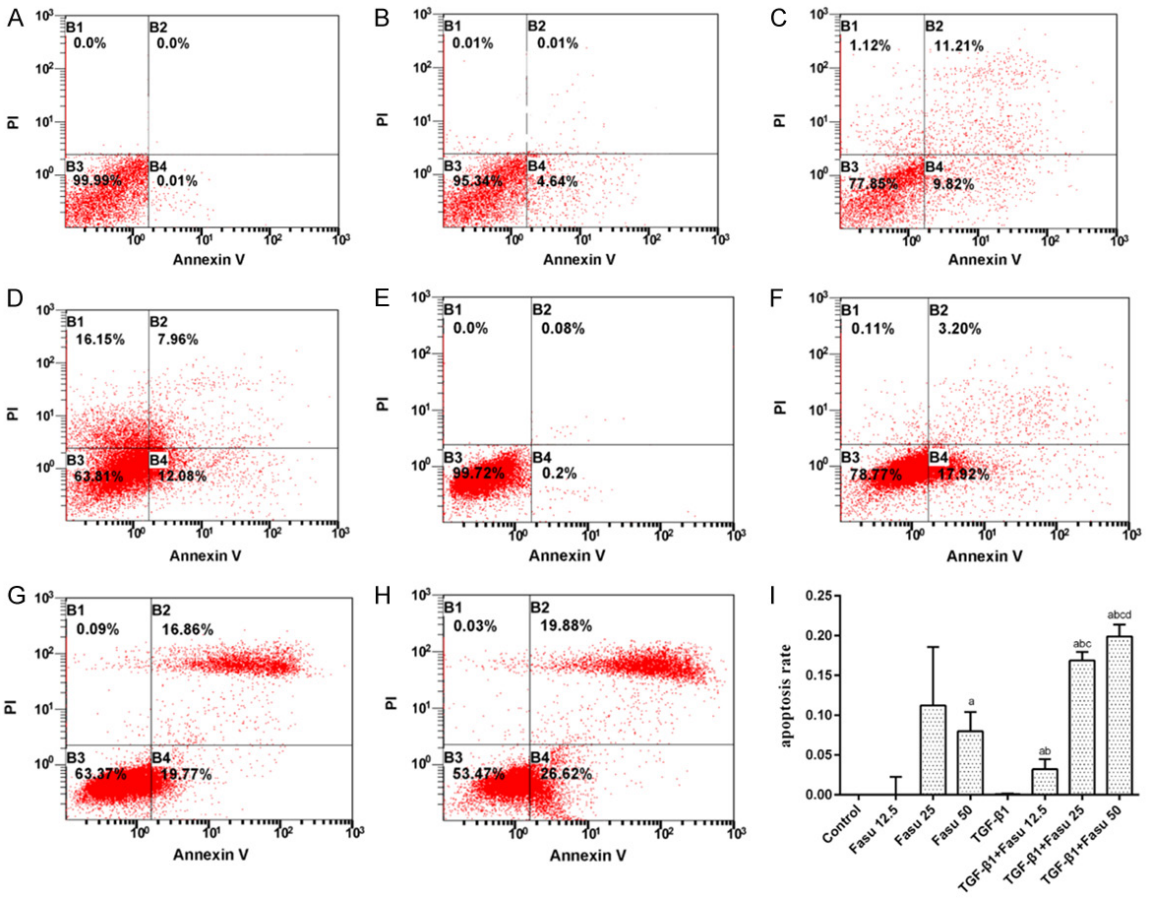

Figure 4. Effects of fasudil on apoptosis of fibroblasts. Cells were treated with different concentrations of fasudil for 24 h. A. Control cells; B. Fasudil 12.5 μmol/L; C. Fasudil 25 μmol/L; D. Fasudil 50 μmol/L; E. TGF-β1; F. TGF-β1+fasudil 12.5 μmol/L; G. TGF-β1+fasudil 25 μmol/L; H. TGF-β1+fasudil 50 μmol/L; I. Apoptosis rate of different group. Data were expressed as mean ± SD (n = 3). [a]$P < 0.05$ cf. control group; [b]$P < 0.05$ cf. TGF-β1 group; [c]$P < 0.05$ cf. TGF-β1 + fasudil 12.5 μmol/L group; [d]$P < 0.05$ cf. TGF-β1 + fasudil 25 μmol/L group.

study, at concentrations of 12.5, 25, and 50 μmol/L, fasudil inhibited fibroblast proliferation in a dose-and time-dependent manner. The IC_{50} concentration for killing fibroblasts was 58.09 and 50.93 μmol/L at 24 and 48 h, respectively. TGF-β1 is known to be involved in the pathogenesis of urethral stricture [23]. In our study, at the doses tested, fasudil also inhibited fibroblast proliferation induced by TGF-β1. The IC_{50} of fasudil inhibition of fibroblast growth with 10 ng/mL TGF-β1 stimulation was 38.49 and 32.95 μmol/L at 24 and 48 h, respectively. These results indicate that the anti-proliferative effect of fasudil is more pronounced in the presence of TGF-β1 stimulation.

A function of apoptosis is the regulation of cell growth. To elucidate further the inhibitory effects of fasudil, we evaluated cell apoptosis via Annexin/PI flow cytometry. The flow cytometry results showed that fasudil reduced the rate of apoptosis in a dose-dependent manner under the stimulation of TGF-β1. However, the urethral scar fibroblasts exposed to concentrations of less than 50 μmol/L fasudil had minimal effects on cell apoptosis in the absence of TGF-β1 stimulation. Higher concentrations of fasudil (50 μmol/L) showed an increase in cell apoptosis without TGF-β1 stimulation. Therefore, the effect of fasudil on cell proliferation was further supported by its promotion of apoptosis.

The main pathology of urethral stricture is the changes in the extracellular matrix of urethral spongiosal tissue. Collagen I and collagen III are the major components of the extracellular matrix. The urethral stricture spongiosum con-

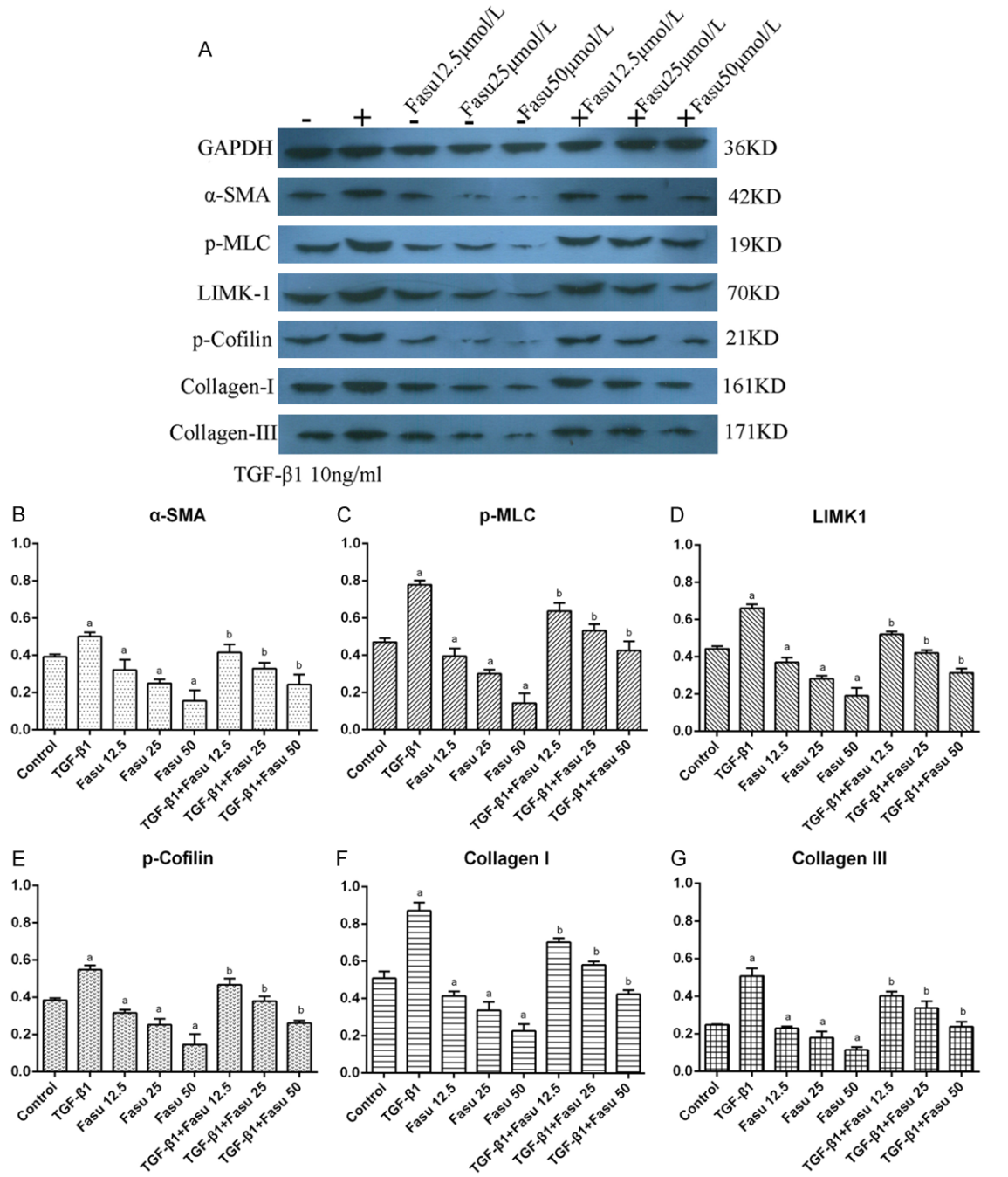

Figure 5. Effects of fasudil on α-SMA, MLCP, LIMK1, p-Cofilin, collagen I, and collagen III protein expression. Protein expression levels were determined by Western blot analysis. A: Showed the reprehensive α-SMA, MLCP, LIMK1, p-Cofilin, collagen I, and collagen III protein band. B-G: Showed the relative α-SMA, MLCP, LIMK1, p-Cofilin, collagen I, and collagen III protein expression to the corresponding GAPDH, respectively. Data were expressed as mean ± SD (n = 3). [a]$P < 0.05$ cf. control group; [b]$P < 0.05$ cf. TGF-β1 group.

sists of 83.9% collagen I and 16.1% collagen III [29]. Our study found overproduction of collagen I and III protein by the urethral scar fibroblasts relative to the control group, particularly in the presence of TGF-β1 stimulation. Treatment with fasudil significantly decreased collagen I and collagen III protein levels in a dose-dependent manner.

Alpha-SMA makes up the basic structure of the cytoskeleton. The fibroblasts transform into myofibroblast-like cells with activation pheno-

types characterized by the expression of α-SMA; α-SMA is specific marker for myofibroblasts. TGF-β1 can promote the transformation of fibroblasts into myofibroblasts [30]. Induction of α-SMA in fibroblasts may promote urethral scar formation [31-33]. In this study, fasudil significantly decreased α-SMA protein expression with or without TGF-β1 stimulation in a dose-dependent manner. Inhibition of the transformation of fibroblasts into myofibroblasts has a key role in reducing pathologic scar formation. In addition, fasudil also decreased fibroblast migration with or without TGF-β1 stimulation, in a dose-dependent manner.

To investigate further the molecular mechanisms of scar formation, we detected proteins that are related to scar formation. ROCK is a major regulator of actin cytoskeleton dynamics downstream of GTPase RhoA [34]. LIMK, cofilin, and MLC are important downstream mediators of ROCK. RhoA and ROCK are considered crucial regulators of scar contracture [35]. Our study showed that activation of MLCP, LIMK1, and p-cofilin protein was detectable in the resting or TGF-β1-stimulated human urethral scar fibroblasts. Activation of MLCP, LIMK1, and p-cofilin proteins may promote the migration of fibroblasts. Treatment with fasudil significantly reduced MLCP, LIMK1, and p-cofilin protein expression. Inhibition of these proteins that are related to scar formation may attenuate urethral scar formation and contraction.

This study suggests that fasudil inhibits proliferation, migration, apoptosis, and collagen synthesis via suppression of the Rho/ROCK pathway. Fasudil may have therapeutic potential in urethral stricture disease.

Acknowledgements

This study was supported by the Young and Middle-Aged Backbone Personnel Training Project of Health System of Fujian Provincial Health and Family Planning Commission (No. 2015-ZQN-JC-20) and Natural Science Foundation of China (No. 81400692).

Disclosure of conflict of interest

None.

Address correspondence to: Dr. Yong Wei, Department of Urology, First Affiliated Hospital of Fujian Medical University, No. 20 Chazhong Road, Fuzhou 350005, China. Tel: +86-059187981687; Fax: +86-059187981687; E-mail: urologyfujian@126.com

References

[1] Santucci RA, Joyce GF and Wise M. Male urethral stricture disease. J Urol 2007; 177: 1667-1674.

[2] Anger JT, Buckley JC, Santucci RA, Elliott SP, Saigal CS; Urologic Diseases in America Project. Trends in stricture management among male Medicare beneficiaries: underuse of urethroplasty? Urology 2011; 77: 481-485.

[3] Bertrand LA, Warren GJ, Voelzke BB, Elliott SP, Myers JB, McClung CD, Oleson JJ, Erickson BA; TURNS. Lower urinary tract pain and anterior urethral stricture disease: prevalence and effects of urethral reconstruction. J Urol 2015; 193: 184-189.

[4] Jackson MJ and Ivaz SL. Quality and length of life, money and urethral stricture disease. Curr Opin Urol 2015; 25: 346-351.

[5] Tritschler S, Roosen A, Fullhase C, Stief CG and Rubben H. Urethral stricture: etiology, investigation and treatments. Dtsch Arztebl Int 2013; 110: 220-226.

[6] Hampson LA, McAninch JW and Breyer BN. Male urethral strictures and their management. Nat Rev Urol 2014; 11: 43-50.

[7] Tian Y, Wazir R, Yue X, Wang KJ and Li H. Prevention of stricture recurrence following urethral endoscopic management: what do we have? J Endourol 2014; 28: 502-508.

[8] Sievert KD, Selent-Stier C, Wiedemann J, Greiner TO, Amend B, Stenzl A, Feil G and Seibold J. Introducing a large animal model to create urethral stricture similar to human stricture disease: a comparative experimental microscopic study. J Urol 2012; 187: 1101-1109.

[9] Yang Y, Yu B, Sun D, Wu Y and Xiao Y. The dose-dependence biological effect of laser fluence on rabbit fibroblasts derived from urethral scar. Lasers Med Sci 2015; 30: 1019-1029.

[10] Cavalcanti AG, Costa WS, Baskin LS, McAninch JA and Sampaio FJ. A morphometric analysis of bulbar urethral strictures. BJU Int 2007; 100: 397-402.

[11] Da-Silva EA, Sampaio FJ, Dornas MC, Damiao R and Cardoso LE. Extracellular matrix changes in urethral stricture disease. J Urol 2002; 168: 805-807.

[12] Jiang HS, Zhu LL, Zhang Z, Chen H, Chen Y and Dai YT. Estradiol attenuates the TGF-beta1-induced conversion of primary TAFs into myofibroblasts and inhibits collagen production and myofibroblast contraction by modulating the smad and Rho/ROCK signaling pathways. Int J Mol Med 2015; 36: 801-807.

[13] Yang R, Chang L, Liu S, Jin X and Li Y. High glucose induces Rho/ROCK-dependent visfatin and type I procollagen expression in rat primary cardiac fibroblasts. Mol Med Rep 2014; 10: 1992-1998.
[14] Zhang XH, Sun NX, Feng ZH, Wang C, Zhang Y and Wang JM. Interference of Y-27632 on the signal transduction of transforming growth factor beta type 1 in ocular tenon capsule fibroblasts. Int J Ophthalmol 2012; 5: 576-581.
[15] Morin P, Wickman G, Munro J, Inman GJ and Olson MF. Differing contributions of LIMK and ROCK to TGFbeta-induced transcription, motility and invasion. Eur J Cell Biol 2011; 90: 13-25.
[16] Hopkins AM, Pineda AA, Winfree LM, Brown GT, Laukoetter MG and Nusrat A. Organized migration of epithelial cells requires control of adhesion and protrusion through Rho kinase effectors. Am J Physiol Gastrointest Liver Physiol 2007; 292: G806-817.
[17] Riento K and Ridley AJ. Rocks: multifunctional kinases in cell behaviour. Nat Rev Mol Cell Biol 2003; 4: 446-456.
[18] Shi J and Wei L. Rho kinase in the regulation of cell death and survival. Arch Immunol Ther Exp (Warsz) 2007; 55: 61-75.
[19] Baba I, Egi Y, Utsumi H, Kakimoto T and Suzuki K. Inhibitory effects of fasudil on renal interstitial fibrosis induced by unilateral ureteral obstruction. Mol Med Rep 2015; 12: 8010-8020.
[20] Qi XJ, Ning W, Xu F, Dang HX, Fang F and Li J. Fasudil, an inhibitor of Rho-associated coiled-coil kinase, attenuates hyperoxia-induced pulmonary fibrosis in neonatal rats. Int J Clin Exp Pathol 2015; 8: 12140-12150.
[21] Zhou H, Zhang KX, Li YJ, Guo BY, Wang M and Wang M. Fasudil hydrochloride hydrate, a Rho-kinase inhibitor, suppresses high glucose-induced proliferation and collagen synthesis in rat cardiac fibroblasts. Clin Exp Pharmacol Physiol 2011; 38: 387-394.
[22] Zhou Y, Huang X, Hecker L, Kurundkar D, Kurundkar A, Liu H, Jin TH, Desai L, Bernard K and Thannickal VJ. Inhibition of mechanosensitive signaling in myofibroblasts ameliorates experimental pulmonary fibrosis. J Clin Invest 2013; 123: 1096-1108.
[23] Sangkum P, Gokce A, Tan RB, Bouljihad M, Kim H, Mandava SH, Saleem SN, Lasker GF, Yafi FA, Abd Elmageed ZY, Moparty K, Sikka SC, Abdel-Mageed AB and Hellstrom WJ. Transforming growth factor-beta1 induced urethral fibrosis in a rat model. J Urol 2015; 194: 820-827.
[24] Zhang Y and Atala A. Urothelial cell culture: stratified urothelial sheet and three-dimensional growth of urothelial structure. Methods Mol Biol 2013; 945: 383-399.
[25] Bei Y, Zhou Q, Fu S, Lv D, Chen P, Chen Y, Wang F and Xiao J. Cardiac telocytes and fibroblasts in primary culture: different morphologies and immunophenotypes. PLoS One 2015; 10: e0115991.
[26] Wang XF, Gao GD, Liu J, Guo R, Lin YX, Chu YL, Han FC, Zhang WH and Bai YJ. Identification of differentially expressed genes induced by angiotensin II in rat cardiac fibroblasts. Clin Exp Pharmacol Physiol 2006; 33: 41-46.
[27] Bae H, Lee D, Kim YW, Choi J, Lee HJ, Kim SW, Kim T, Noh YH, Ko JH, Bang H and Lim I. Effects of hydrogen peroxide on voltage-dependent K(+) currents in human cardiac fibroblasts through protein kinase pathways. Korean J Physiol Pharmacol 2016; 20: 315-324.
[28] Chong T, Fu DL, Li HC, Zhang HB, Zhang P, Gan WM and Wang ZM. Rapamycin inhibits formation of urethral stricture in rabbits. J Pharmacol Exp Ther 2011; 338: 47-52.
[29] Baskin LS, Constantinescu SC, Howard PS, McAninch JW, Ewalt DH, Duckett JW, Snyder HM and Macarak EJ. Biochemical characterization and quantitation of the collagenous components of urethral stricture tissue. J Urol 1993; 150: 642-647.
[30] Park IH, Park SJ, Cho JS, Moon YM, Moon JH, Kim TH, Lee SH and Lee HM. Effect of simvastatin on transforming growth factor beta-1-induced myofibroblast differentiation and collagen production in nasal polyp-derived fibroblasts. Am J Rhinol Allergy 2012; 26: 7-11.
[31] Sa Y, Li C, Li H and Guo H. TIMP-1 induces alpha-smooth muscle actin in fibroblasts to promote urethral scar formation. Cell Physiol Biochem 2015; 35: 2233-2243.
[32] Mack M and Yanagita M. Origin of myofibroblasts and cellular events triggering fibrosis. Kidney Int 2015; 87: 297-307.
[33] Darby IA, Laverdet B, Bonte F and Desmouliere A. Fibroblasts and myofibroblasts in wound healing. Clin Cosmet Investig Dermatol 2014; 7: 301-311.
[34] Loirand G. Rho kinases in health and disease: from basic science to translational research. Pharmacol Rev 2015; 67: 1074-1095.
[35] Bond JE, Kokosis G, Ren L, Selim MA, Bergeron A and Levinson H. Wound contraction is attenuated by fasudil inhibition of Rho-associated kinase. Plast Reconstr Surg 2011; 128: 438e-450e.